Green Heterogeneous Base Catalyst from Ripe-Unripe Plantain Peels for the Transesterification of Waste Cooking Oil

Olayomi Abiodun Falowo (falowo.olayomi@lmu.edu.ng)
Landmark University College of Science and Engineering https://orcid.org/0000-0003-2123-0676
Babatunde Oladipo
Cape Peninsula University of Technology Faculty of Engineering
Abiola Ezekiel Taiwo
Landmark University
Tomiwa Ayomiposi Olaiya
Landmark University
Oluwaseun Oyekola
Cape Peninsula University of Technology Faculty of Engineering
Eriola Betiku
Obafemi Awolowo University Faculty of Technology

Research Article

Keywords: Transesterification, Taguchi, Waste cooking oil, Biodiesel, Plantain peels, Catalyst

Posted Date: December 21st, 2021

DOI: https://doi.org/10.21203/rs.3.rs-1136793/v1

Abstract

Economical feedstocks such as agricultural wastes, food wastes, and waste cooking oil were used for biodiesel production to expand their application. Thus, a solid base catalyst was synthesized from a mixture of ripe and unripe plantain peels at a calcination temperature of 500 ^{o}C for 4 h. The catalyst was characterized using Scanning Electron Microscope (SEM), X-ray Diffraction (XRD) analysis, Fourier Transform Infrared (FT-IR) spectroscopy, Energy dispersive X-ray (EDX) analysis, and Brunauer-Emmett-Teller (BET) method. The waste cooking oil (WCO) used in this study was first pretreated with 3% (v/v) of H_2SO_4 via esterification reaction due to its high acid value. The esterified WCO was converted to biodiesel via transesterification reaction, and the process was then modeled and optimized using Taguchi L9 orthogonal array design method considering reaction temperature, reaction time, catalyst amount, and methanol/WCO molar ratio as the input variables. Based on the results, the synthesized catalyst predominantly contained potassium phases with 45.16 wt.%. The morphology of the catalyst revealed a crystalline mesoporous nanocomposite. At the end of WCO esterification, the acidity of the oil decreased from 5 to 1 mg KOH/g. The optimal conditions established for the transesterification process were catalyst amount of 0.5 wt.%, methanol/WCO molar ratio of 6:1, reaction temperature of 45 ^{o}C, and reaction time of 45 min with a corresponding biodiesel yield of 97.96 wt.%. The quality of the biodiesel produced satisfied the specifications (ASTM D6751 and EN 14241) recommended for biodiesel fuels. Hence, a blend of ripe and unripe plantain peels could serve as an efficient heterogeneous base catalyst in producing biodiesel from WCO.

1. Introduction

The petroleum oil price and the environmental pollution generated from fossil fuels have made biofuel production a developing area. Other alternative non-polluting technologies such as hydrogen-fueled vehicles, hybrids, plug-in electrics, compressed natural gas, and solar enable devices are possible solutions to energy and environmental problems (Kumar and Sharma, 2011). However, biofuels are renewable energy sources with vast potentials to replace fossil fuels in the present and future energy mix (Deora et al., 2021). Biomass sources from which biofuels are naturally abundant and can ensure the stability of the ecosystem. Biodiesel, a form of biofuel, is a renewable source of energy with several environmental benefits.

The methods involved in producing biodiesel depend on the catalyst used in the process. Different catalysts that have deployed in producing biodiesel are base catalysts (e.g., KOH or NaOH), acid catalysts (e.g., H_2SO_4), and enzymes (e.g., lipases) (Marchetti et al., 2007). Currently, investment in biodiesel production is adversely affected by several factors including, production technology type, nature of raw materials, and market feedstocks price (Gebremariam and Marchetti, 2018). Biodiesel price doubles that of mineral diesel in the market, due to its production cost. Biodiesel production cost involves two parts, viz., raw materials (feedstocks) cost and processing cost (Huang et al., 2010).

It is argued that the biodiesel production cost depends on the technological routes; however, the cost of feedstock, regardless of the technology employed, accounts for the major production costs (Akella et al., 2009; Ahmad et al., 2011). To produce economical biodiesel would require a cheap source of feedstock such as inedible oil, used cooking oil, and animal fats (Gebremariam and Marchetti, 2018). Generally, non-edible oils are not consumed by humans due to the presence of toxic compounds. Also, their availability and the low cost of

plantation of non-edible oil crops position them as economically viable feedstocks. However, many non-edible oils are not suitable for biodiesel synthesis and require pretreatment (Gebremariam and Marchetti, 2018; Deora et al., 2021). Several developed countries, due to climate change threats, are embracing alternative energy sources. The increasing interest in biofuel is due to its intrinsic advantages over fossil fuels. To this effect, the growth projection of the biodiesel industry may place huge pressure on nature and biodiversity in emergent nations (Kumar and Sharma, 2011). One way to address this pending crisis is to adopt total biomass-dependent fuel. Waste cooking oil is a good raw material for biodiesel development since it is cheap and abundant in several countries. Its usage in biodiesel synthesis will prevent competition from using edible oils (Soji-Adekunle et al., 2018; Sivarethinamohan et al., 2022). Apart from the converting waste cooking oil (WCO) to fuel, the problems associated with its disposal are equally solved (Predojević, 2008). It is estimated that a minimum of 16.54 million tons of WCO is produced every year, covering major countries in Europe, Asia, and North America (Loizides et al. (2019).

Conventionally, biodiesel is industrially produced using homogeneous catalysts. The use of homogeneous catalysts for the transesterification of triglycerides is not friendly to the environment and equipment, while the enzymatic transesterification process is expensive (Balajii and Niju, 2019; Bhatia et al., 2020). The use of solid catalysts for biodiesel production has several advantages: minimum energy consumption, lower material costs, and minimum water usage. This class of catalysts can easily be separated from the product and recycled many times (Betiku et al., 2016; Oladipo et al., 2018). Green catalysts are mostly derived from biomass resources such as plants or animals (Qiu et al., 2011; Betiku et al., 2017). Catalysts from natural biological sources contain calcium and potassium compounds dominantly. These elements are potential solid base catalysts for the transesterification of triglycerides (Betiku et al., 2016; Abdullah et al., 2017). The production of green catalysts involves a sequence of easy methods with minimal energy requirements (Odude et al., 2017). Previous studies have reported different plant biomass in producing solid catalysts employed in the transesterification reaction (Sharma et al., 2012; Oladipo et al., 2018). The rationale is to discover abundant plant biomass of high catalytic properties which can be efficiently used sustainably. Previous reports have demonstrated the use of banana and plantain wastes. These include *Musa Balbisiana* colla trunk (Deka and Basumatary, 2011), plantain peels (Betiku and Ajala, 2014), banana peels (Betiku et al., 2016), *Musa Balbisiana* Colla peels (Gohain et al., 2017), *Musa acuminate* (Balajii and Niju, 2019) peduncle, and banana peduncle (Balajii and Niju, 2020). Also, a mixture of plant biomass has been used to develop solid catalysts; cocoa pod husk-plantain peel (Olatundun et al., 2020) and cocoa pod husks-plantain peel-kola nut husk (Falowo et al., 2020).

This study reports the synthesis of a green solid catalyst from agricultural wastes and its subsequent application in the transesterification reaction. The focus was to produce biodiesel from WCO via transesterification using the base catalyst developed from ripe and unripe plantain peels mixture. The heterogeneous base catalyst was synthesized from a mixture containing an equal proportion of ripe and unripe plantain peels ashes. The biodiesel yield and the process parameters (reaction time, molar ratio of oil to methanol, reaction temperature, and catalyst loading) influencing the process were investigated using the Taguchi approach. The optimization of the transesterification of WCO was carried out to maximize the utilization of raw materials, and hence, lessen the production cost.

2. Materials And Methods

2.1 Materials

The WCO, together with the ripe and unripe plantain peels used in this study, were obtained from the Cafeteria Kitchen of Landmark University, Omu-Aran, Kwara State, Nigeria. Analytical grade reagents and chemicals were used for the study.

2.2 Synthesis of catalyst from plantain peels

The two types of plantain peels used in this study were treated separately before calcination. The ripe and unripe plantain peels collected were cut into small pieces, then washed in distilled water to remove the dirt and stones. The washed peels were oven-dried at 100 ^{o}C until a constant weight was observed. The plantain peels were burnt, and the resultant ashes were mixed in equal proportion (ripe:unripe of 50:50). The mixed powdered ash was loaded in the porcelain crucible and calcinated in the muffle furnace at 500 ^{o}C for 4 h, according to Betiku and Ajala (2014). After calcination, the calcined ripe-unripe plantain ash (CRUPA) was sieved using 80 mesh size, and the obtained ash was stored for further work.

2.3 Characterization of CRUPA

The synthesized catalyst was characterized to investigate its features. Energy-dispersive X-ray spectroscopy (EDS) of CRUPA was performed to determine the elemental contents using a Thermo Fisher Nova NanoSem, and the diffractogram generated was recorded with an Oxford X-max 20mm^2 detector (Oxfordshire, U.K.) The functional groups on the active site of the CRUPA surface were determined by Fourier Transform Infrared (FTIR) analysis using a Perkin Elmer UATR Two spectrophotometer (Llantrisant, U.K.). The spectra generated were recorded over the range of 4000 to 400 cm^{-1}. The crystalline phases in CRUPA were determined using X-ray diffractometer D8-Advance from Bruker AXS (Germany). The measurement involves a continuous scan in locked coupled mode with Cu-K_a radiation with LynxEye detectors. The sample measurements run within a range of 2θ with a typical step size of 0.034° in 2θ. The surface morphological features of CRUPA were taken using Tescan MIRA3 RISE scanning electron microscopy (SEM). The Brunauer-Emmett-Teller (BET) method of adsorption/desorption on nitrogen gas was used to determine the surface area and porosity of CRUPA using a Micromeritics instrument (Tristar II 3020). The catalyst pore size distribution, width, and adsorption pore volume were determined by Barret-Joyner-Halenda (BJH) method.

2.4 Pretreatment of WCO

WCO was centrifuged to remove the solid residues and particles left after being used. Thereafter, the oil was moderately heated to evaporate any water moisture that might be trapped. After cooling, the physicochemical properties of WCO (acid value, density, kinematic viscosity, saponification value, and iodine value) were measured according to the standard methods (AOAC, 1990). The physicochemical characterization of the WCO had an acid value of 5 mg KOH/g oil. Hence, WCO was subjected to the esterification process to reduce its acid value (Betiku et al., 2017). The esterification of WCO was carried out in a two-neck glass reactor placed on a hotplate with a magnetic stirrer. The esterification conditions were methanol/WCO molar of 6:1, temperature of 65 ^{o}C, reaction time of 45 min, and catalyst amount of 3% (v/v). A known volume of WCO was measured, and methanol of known volume was added. The esterification process proceeds accordingly. After the process, the esterified oil was separated using a centrifuge (TMT-XC-450-PRP) machine. The esterified oil was dried over a hotplate and stored for further use.

2.5 Transesterification of WCO using CRUPA

The transesterification of WCO and methanol using a synthesized catalyst (CRUPA) was carried out according to the conditions stipulated by Taguchi orthogonal array (L9) design method. The L9 design was chosen for its simplicity and ability to provide exhaustive information about the process parameters and the yield using a few experiments (Oraegbunam et al., 2020). The parameters considered in the modeling of WCO transesterification are methanol-to-WCO molar ratio, temperature, time, and catalyst amount. The chosen parameters were based on our previous studies (Oladipo et al., 2020; Fadara et al., 2021). The different levels of each parameter used in this study are methanol-to-WCO molar ratio (6:1, 9:1 and 12:1), reaction temperature (45, 55 and 65 ^{o}C), reaction time (50, 70 and 90 min) and catalyst loading (0.5, 1.5 and 2.5 wt.%).

Biodiesel production from WCO was conducted in a three-necked glass reactor placed on a hotplate with a magnetic stirrer. A glass reflux condenser was mounted on the reactor to prevent methanol evaporation from the reaction mixture. Initially, a known volume of WCO was charged into the glass reactor, a known amount of methanol was added to it depending on the molar ratio specified. The mixture was allowed to heat to the set temperature under continuous stirring. Then, a known amount of CRUPA was added, and the reaction continued for a time suggested by the model. After the transesterification process, the mixture was centrifuged to separate methanol, biodiesel, and the residual catalyst. The biodiesel was washed three times with warm distilled water (65 ^{o}C) to remove impurities and residual methanol. The biodiesel obtained (waste cooking oil methyl esters - WOME) was dried, and the yield was gravimetrically determined using Eq. (1).

$$Biodiesel\ yield = \frac{weight\ of\ WOME\ produced}{weight\ of\ WCO\ used} \times 100 \qquad (1)$$

2.6 Physicochemical properties of WOME

The quality of WOME produced was ascertained by determining the physicochemical properties of the fuel. The specific gravity, saponification value, acid value, density, iodine value, and kinematic viscosity were determined using the standard method (AOAC, 1990). Other fuel parameters such as cetane number (Krisnangkura, 1986) and calorific value (Demirbaş, 1998) were also determined. The FTIR analysis of WOME was carried out using an FTIR-UATR spectrophotometer.

3. Results And Discussion

3.1 Characterization results of CRUPA

3.1.1 Elemental composition of CRUPA

The chemical composition obtained using EDX analysis at five different sites is shown in Figure 1. The mean (wt.%) of the elemental composition of CRUPA is presented in Table 1, and the elements present are C, O, Mg, Si, and K. The results show a considerable presence of potassium (K) in the form of K_2O and K_2CO_3 as well as other traces of metallic oxides. This indicates that the developed CRUPA has high basicity due to the presence of metallic oxide. As a result, the synthesized catalyst could be an efficient heterogeneous catalyst in expediting

the transesterification of biomass oil. The K content (45.16 wt.%) in this study was more than the K value (41.37 wt.%) found in the calcined banana peel ash (Gohain et al., 2017). However, a higher K content was earlier reported in previous studies that used either ripe plantain peels or unripe plantain peels. The K content (54.73 wt.%) was reported for a calcined sample (temperature: 500 ^{o}C) developed from unripe plantain peels (Betiku and Ajala, 2014). Balajii and Niju (2020) reported K (68.37 wt.%) as the major element in the banana peduncle calcined at 700 ^{o}C, other elements such as Mg, Ca, O were present. Similarly, Etim et al. (2018) reported K (51.02 wt.%) as the dominant element, and the presence of elements such as O, P, Ca, Mg, S, Cl, Al, and Si in the calcined ripe plantain peels at 700 ^{o}C. The observed difference in the elemental constituent could be attributed to the calcination temperature used, and the blending of ripe and unripe plantain peel ashes.

Table 1. Elemental constituents of CRUPA

Composition	C	O	Mg	Si	K
	(%wt. fraction)				
Mean value	12.02	35.34	3.61	3.87	45.16
Standard deviation	4.5	3.68	1.61	1.76	2.79

3.1.2 FT-IR results of CRUPA

FT-IR spectroscopy was used to identify the vibration of chemical bonds in the analyzed sample. Each vibration uniquely describes a certain functional group; hence, the feature of the spectrum gives structural information on the catalyst molecules. The FT-IR spectrum of CRUPA is shown in Figure 2. The absorption vibration at 1380 cm^{-1} was assigned to asymmetric stretching of carbonate functional group while the band at 900 cm^{-1} was due to out-of-plane bending vibration of the C-O group (Betiku et al., 2017; Pavlović et al., 2020), hence, indicating the presence of carbonate compound (K_2CO_3) which has been identified around this band (Sharma et al., 2012). The band around 1430 cm^{-1} can be ascribed to atmospheric CO_2 adsorption onto metal oxide (Balajii and Niju, 2020). The absorption at 1000 cm^{-1} can be attributed to Si-O-Si vibration, which is prominent in the calcined material (Gohain et al., 2017). The weak adsorption around 3100–2900 cm^{-1} may be assigned to M-K-O group, where (M = Mg or Si). The results in this section corroborate the EDX results.

3.1.3 XRD results of CRUPA

The bulk phases of the CRUPA were identified using XRD analysis. The XRD peak of the synthesized catalyst is depicted in Figure 3. According to the results, the two phases identified in this catalyst are potassium chloride (KCl) and potassium carbonate hydrate ($K_2CO_3 1.5H_2O$).

The lattice structure of KCl was face-centered cubic while that of potassium carbonate hydrate was monoclinic. The XRD pattern of KCl phase showed clear diffraction peaks at 2θ = ∼15, 28, ∼42, 50, and 67 while $K_2CO_3 1.5H_2O$ exhibits strong intensity at 2θ = 26, 30, 33, 40, and 43. In the XRD diffractogram of calcined banana peels, KCl and $K_2CO_3 1.5H_2O$ are the dominant two crystalline phases (Betiku et al., 2016). Meanwhile, different crystalline compounds were identified in calcined ripe plantain peels (Etim et al., 2018). Only KCl was among the crystalline phases.

3.1.4 SEM results of CRUPA

The surface morphology of CRUPA was examined by scanning electron microscope. The SEM images of the catalyst taken at different nano-sizes are shown in Figure 4(a-d), which revealed the microstructure similar to the morphology earlier reported (Betiku et al., 2016; Olatundun et al., 2020). Figure 4a shows a large aggregate of spherical particles clumped together. The SEM image at (4b) shows increasing agglomerated particles with regular size distribution. The SEM image becomes clearer in (4c) with a highly ordered surface with large cracks across the image. At 10μm (4d), the porosity of CRUPA was highly noticeable, having a glossy-like surface.

3.1.5 Surface area, pore-volume, and pore width of CRUPA

The synthesized catalyst (CRUPA) had a BET surface area of 1.10 ± 0.0050 m^2/g, pore volume of 0.002366 cm^3/g, and pore size width of 13.15 nm. The surface area compared favorably to the earlier reported results; 1.487 m^2/g from *Musa Balbisiana* trunk (Deka and Basumatary, 2011). The BET isotherm of CRUPA is displayed in Figure 5a. The adsorption isotherm exhibited by CRUPA is a typical Type IV isotherm. This means that adsorbate would condense in the tiny capillary of the catalyst at a pressure below saturation pressure of the gas (Hwang and Barron, 2011). At the lower pressure, the inflection region represents monolayer formation while capillary condensation or multilayer formation occurs after monolayered surface coverage of the pore walls (Hwang and Barron, 2011; Naderi, 2015). The adsorption of the adsorbate on the pore surface steadily increases until it jumps at the relative pressure (P/P_0) equals 0.9. The BJH pore-size distribution of CRUPA is depicted in Figure 5b. The plot exhibits a strong interaction between adsorbate and calcined sample surface between the pore diameters of 5–25 nm. The synthesized catalyst in this study can be classified as a mesoporous material, that is, material or particles having a pore diameter within 2–50 nm (Naderi, 2015; Falowo et al., 2020).

3.2 Results of WCO transesterification

The pretreatment of high acid value oil is essential in producing biodiesel (Olagbende et al., 2021). The esterification reaction of WCO using H_2SO_4 as a catalyst proved effective in reducing the %FFA of the oil 5 mg KOH/g oil to 1 mg KOH/g oil, which meant that 80% FFA reduction was achieved within the experimental conditions. The esterified WCO was directly transesterified to biodiesel since its acid value was within an allowable range. The actual yields and predicted biodiesel yields obtained from the transesterification of WCO under 9 experimental conditions are presented in Table 2.

Table 2. Taguchi model of actual and predicted biodiesel yield

Run	A: MeOH/WCO ratio	B: Temp. ^oC	C: Cat. loading wt.%	D: Time min	Actual WOME wt.%	Predicted WOME wt.%
1	9:1	65	0.5	70	62.37	62.49
2	9:1	45	1.5	90	66.02	65.98
3	9:1	55	2.5	50	60.35	60.27
4	6:1	65	2.5	90	90.56	90.48
5	6:1	45	0.5	50	96.39	96.51
6	6:1	55	1.5	70	87.34	87.31
7	12:1	65	1.5	50	81.94	81.90
8	12:1	55	0.5	90	76.07	76.19
9	12:1	45	2.5	70	84.51	84.43

It was observed that the actual and predicted biodiesel yields are comparable, demonstrating the accuracy of the model in predicting the responses. Run 5 at the lowest level of the operating parameters gave the highest biodiesel yield of 96.39 wt.%. The lowest biodiesel yield (60.35 wt.%) was recorded at run 3, with the lowest reaction time, the upper level of catalyst loading, and the middle level of temperature and methanol/oil molar ratio. The results obtained from the transesterification of WCO were fitted into the Taguchi L9 orthogonal array model response. An analysis of variance (ANOVA) was used to optimize the experimental results to determine the relative influence of process parameters considered. The p-value of the model and each parameter at a 95% confidence level (p-value $\leq$ 0.05) was used to determine the significance of these terms. From the results (Table 3), the model is significant, including the methanol/WCO molar ratio, temperature, and reaction time. The impact of catalyst loading on the transesterification process cannot be captured statistically; hence, it is insignificant within the range investigated. It was observed that there is a 0.01% chance of getting this high F-value (1342.92) due to noise. The relative contribution of the individual parameter was quantified by the ratio of the pure sum of squares to the total sum of squares. The methanol/WCO molar ratio is the most influential parameter, followed by temperature. Also, reaction time had minimal effect on the biodiesel yield since it has the lowest F-value among the parameters investigated.

Table 3. ANOVA results of model and process parameters

Source	Sum of Squares	Degree of freedom	Mean Square	F-value	p-value
Model	1342.92	6	223.82	6880.67	0.0001
A-MeOH/WCO	1247.01	2	623.51	19167.85	< 0.0001
B-Temperature	89.37	2	44.68	1373.69	0.0007
D-Time	6.54	2	3.27	100.47	0.0099
Residual	0.0651	2	0.0325		
Cor Total	1342.98	8			

The linear regression model in terms of coded factors that described the transesterification of WCO is presented in Eq. (2). This model equation is useful in predicting biodiesel yield at a given level of each parameter.

$$WOME = +78.39 + 13.04A[1] - 15.48A[2] + 3.91B[1] - 3.81B[2] - 1.17D[1] - 0.32D[2] \quad (2)$$

where A[1] and A[2] represent methanol/WCO molar ratio at 1st and 2nd level, B[1]and B[2] represent the temperature at 1st and 2nd level, while D[1] and D[2] are the reaction time at 1st and 2nd level, respectively. The relative impact of an individual parameter on the yield can be identified by comparing the coefficient of the regression equation.

The statistical fitness of this model was evaluated (Table 4). The coefficient of determination (R^2) in this study was 0.9998, which indicates that the experimental data obtained from the chosen model fitted perfectly. The R^2 value is close to 1, an indication that 99.98% of the variation observed in biodiesel yields with respect to the process parameters can be explained by the model. The adjusted R^2 and predicted R^2 values are 0.9993 and 0.9990, respectively. These values are in reasonable agreement with one another and less than the maximum allowable difference of 0.2. The standard deviation of this analysis was 0.1804, which shows that the results

obtained from this study are reliable. The coefficient of variation (C.V. %) was 0.2301; the lower the value, the better the capability of the model in optimizing the process (Dhawane et al., 2016). The adequate precision of the model was 227.82; a value greater than 4 is considered adequate (Olagbende et al., 2021). Meanwhile, the value obtained is very high, which indicates that the model has sufficient signal to optimize the transesterification of WCO.

Table 4
Quality of statistical parameters

Parameters	Value
Standard deviation	0.1804
Mean	78.39
Coefficient of Variation (%)	0.2301
R^2	0.9998
Adjusted R^2	0.9993
Predicted R^2	0.9990
Adequate precision	227.8172

3.3 Parametric influence of reaction parameters

3.3.1 Effect of methanol/WCO molar ratio on WOME yield

The influence of methanol/WCO molar ratio on WOME yield at a temperature of 45 ^{o}C, reaction time of 50 min, and 0.5 wt.% catalyst loading is displayed in Figure 7. Generally, transesterification reaction according to the stoichiometric ratio requires a methanol/oil molar ratio of 3:1. However, excess methanol is needed to shift the equilibrium position to favour forward reaction. In this study, maximum biodiesel yield (96.39 wt.%) was reached at a methanol/oil molar ratio of 6:1. Oladipo and Betiku (2020) obtained 96.97 wt.% of *Hevea brasiliensis* oil methyl ester using a methanol/oil molar ratio of 6:1. Increasing the molar ratio to 9:1 led to a sharp reduction in biodiesel yield. The reason could be due to excessive dilution of oil by the methanol, thereby decreasing the rate of transesterification reaction (Zhang et al., 2019). A marginal increase in biodiesel yield was observed when the molar ratio was later increased to 12:1. A similar observation was reported in Oraegbunam et al. (2020), the maximum biodiesel yield was reached at a methanol/oil molar ratio of 6:1, and excess methanol to the reaction mixture led to a reduction in biodiesel yield. Excess methanol was reported to have increased glycerol solubility, which interferes with the ester phase and subsequently lowers biodiesel yield (Predojević, 2008).

3.3.2 Effect of reaction temperature on WOME yield

The influence of temperature on WOME yield at methanol/WCO molar ratio of 6:1, catalyst loading of 0.5 wt.%, and reaction time of 50 min is depicted in Figure 7. The biodiesel yield was at the peak at the lowest level of the temperature (45 ^{o}C). It can be seen that the biodiesel yield decreased when the temperature was increased, and

the yield again marginally increased with a further increase in temperature to 65 ^{o}C. The response of biodiesel yield to changes in temperature demonstrated the effect of temperature on the equilibrium constant of the transesterification process. The influence of temperature observed in this study aligns with earlier studies. Soji-Adekunle et al. (2018) reported that biodiesel yield decrease with an increase in reaction temperature. The authors produced a maximum biodiesel yield of 94 wt.% at a temperature of 55 ^{o}C. Similarly, a biodiesel yield of 96.43 wt.% was obtained at the reaction temperature of 35 ^{o}C. A marginal increase in biodiesel yield was observed at the reaction temperature (65 ^{o}C) close to the boiling point of methanol. This could be attributed to the turbulence in the system, which subsequently strengthens the mass transfer rate of reacting molecules (Zhang et al., 2019).

3.3.3 Effect of reaction time on WOME yield

The impact of reaction time on the WOME yield at methanol/WCO molar ratio of 6:1, a temperature of 45 ^{o}C, and 0.5 wt.% CRUPA is shown in Figure 8. At the lowest level of reaction time, 96.39 wt.% of biodiesel yield was obtained. Further increment in reaction time led to a marginal reduction in biodiesel yield. According to the results, increasing the reaction time from 70 to 90 min at a constant temperature, CRUPA loading, and MeOH/WCO molar ratio had minimal effect on the biodiesel yield. Oladipo et al. (2020) reported that 40 min was sufficient to produce 96.53 wt.% of biodiesel from moringa oil. Since transesterification is a reversible reaction (Ma and Hanna, 1999), produced biodiesel can be converted to triglycerides at a longer reaction time. This could be the reason the biodiesel yield decreases with increasing reaction time.

3.4 Establishment of optimal condition and model validation

The optimal condition for the transesterification of WCO to WOME by CRUPA was established using the numerical optimization method of solving the regression model. The optimum values predicted were catalyst loading of 0.5 wt.%, methanol/WCO molar ratio of 6:1 (v/v), temperature of 45 ^{o}C, and reaction time of 45 min with a corresponding biodiesel yield of 97.96 wt.%. The performance of the model was validated by conducting the transesterification of WCO under optimum conditions predicted by the regression model. The experiment at the optimum values was repeated thrice, and the average value of biodiesel yield obtained was 97.52 wt.%. The average biodiesel yield is close to the predicted biodiesel yield, which signifies that the model used in this study is capable of predicting the optimum values and adequately describes the process.

3.5 Results of CRUPA reusability

One of the advantages of the heterogeneous catalyst over the homogeneous catalyst is recycling the catalyst and reapplying it in another production cycle. The reusability test was conducted to determine the number of production cycles this catalyst can be reused. This test was conducted at the optimum conditions of the model. At the end of each run, the solid catalyst was separated and applied to another transesterification set-up without any treatment. A plot of biodiesel yields against production run is presented in Figure 9. It was observed that the synthesized catalyst could be reused for five production cycles without losing a substantial amount of biodiesel. At the end of the 5th cycle, the biodiesel yield was reduced by 13.32%. The loss of catalytic activity of the catalyst can be attributed to partial blocking of catalyst pores by reacting molecules which subsequently prevent other triglyceride molecules from accessing the active catalyst surface (Konwar et al., 2014).

3.6 FT-IR spectrum of WOME

The FT-IR spectrum of the WOME is shown in Figure 10. The absorption bands present and the corresponding vibrational types are depicted in Table 5. The stretching vibration of the hydroperoxide functional group was assigned to the weak band at 3422 cm^{-1}. The two strong absorption bands that characterized the presence of ester: the carbonyl group (–C=O 1745 cm^{-1}) and anti-symmetric axial stretching (–C–O–C) (Tariq et al., 2011; Falowo et al., 2019) are present. The signals at 2928 and 2854 cm^{-1} are assigned to the asymmetric and symmetric stretching vibration, respectively (Qiu et al., 2011; Falowo et al., 2019). Thus, the FT-IR spectrum obtained indicates that the transesterified WCO possessed characteristics signals of fatty acid methyl esters, which confirms that the transesterification process was successful.

Table 5
Wavenumber and vibration types present in WOME

Wavenumber (cm^{-1})	Functional group	Vibration type	References
3422	-O-H	Stretching	(Qiu et al., 2011; Olatundun et al., 2020)
2928	$-CH_2$	Asymmetric stretching vibration	(Mustata and Bicu, 2014; Oladipo et al., 2020)
2854	$-CH_2$	Symmetric Stretching vibration	(Falowo et al., 2019; Olatundun et al., 2020)
1745	-C=O	Carbonyl stretching vibration	(Tariq et al., 2011; Oladipo et al., 2020)
1460	$-CH_2$	Shear-type vibration	(Sharma et al., 2012; Konwar et al., 2014)
1174	-C-O-C	Anti-symmetric stretching vibration	(Tariq et al., 2011; Mustata and Bicu, 2014)
721	$-CH_2$	Plane rocking vibration	(Konwar et al., 2014; Fadara et al., 2021)

3.7 Physicochemical properties of WOME

The physical and chemical properties of WCO and biodiesel produced using CRUPA were characterized, and the results, along with the recommended standards (ASTM D6751 and EN 14214) for biodiesel, are presented in Table 6. Based on the results, there was an improvement in the physicochemical properties of the biodiesel over WCO. This further highlights the importance of the transesterification in the conversion of triglycerides to methyl esters. The acid value of WOME synthesized in this study compared with the value reported in other studies (Soji-Adekunle et al., 2018; Gohain et al., 2020) indicates that the biodiesel is stable and will minimize the deposit rate in the fuel system. The kinematic viscosity, cetane number, calorific value, and density of the produced WOME show that the biodiesel has a good ignition quality and sufficient energy capacity. The values also compared favorably with the biodiesel produced from WCO using different catalysts and the values recommended for biodiesel standards.

Table 6. Properties of biodiesel synthesized from waste cooking oil using different catalysts

Properties	Unit		This study	Gohain *et al.* (2020)	Niju *et al.* (2019)	Soji-Adekunle *et al.* (2018)	Standards	
		WCO	CRUPA	Calcined pawpaw stem	Calcined sugarcane bagasse	KOH	EN 14214	ASTM D6751
Density (25 °C)	kg/m^3	981	890	870	878	852	860 - 900	880
Acid value	mg KOH/g oil	5.65	0.46	0.06	0.45	0.32	0.5 max	0.5 max
Kinematic viscosity	mm^2/s	6.22	3.90	3.10	4.75	5.87	3.5 - 5	1.9 - 6
Iodine value	g I_2/100g oil	122.02	71.28	-	-	74.67	120	NS
Flash point	^oC	-	-	150	158	176	-	-
Saponification value	mg KOH/g	186.45	154.5	-	-	58.10	NS	NS
Cetane number	-	48.19	60.12	57	-	58.64	51 min	47 min
Calorific value	MJ/kg	39.97	42.34	40.30	-	45.93	35	NS

4. Conclusion

The utilization of biodiesel in the energy mix has been reported to guarantee energy security and ensure ecological balance. Biodiesel production on a large scale, if to be economical, would require inexpensive, abundant biomass as feedstock. A mixture of ripe and unripe plantain peels used in synthesizing solid base catalyst is a viable feedstock. The catalyst (CRUPA) had high catalytic properties to transesterify WCO to biodiesel. The synthesized solid base catalyst predominantly contains potassium compounds; the K content was 45.16 wt.%. Factors such as temperature, reaction time, catalyst loading, and methanol/oil molar ratio affect the response of the transesterification process. The optimal condition established for WOME production from WCO using CRUPA was catalyst loading of 0.5 wt.%, methanol/oil molar ratio of 6:1, a temperature of 45 ^oC, and reaction time of 45 min, with a corresponding biodiesel yield of 97.96 wt.%. The biodiesel produced (WOME) had physicochemical properties which met biodiesel standards (ASTM D6751 and EN 14241). Thus, a blend of calcined ripe-unripe plantain peels could be utilized as an efficient heterogeneous catalyst for biodiesel production.

Declarations

Acknowledgement

The authors appreciate the technologists in the Department of Chemical Engineering, Landmark University, Omu-Aran, Nigeria.

Ethical Approval

The research results presented in this manuscript are the original works of the authors. This paper has not been published elsewhere in any form or language. The manuscript has not been submitted to another journal for consideration. Authors of this work have presented their results clearly without any falsification or misrepresentation of data. All references used in this study were properly acknowledged and all rules guiding a good scientific practice were maintained to ensure professionalism.

Consent to participate

Not applicable

Consent to publish

Not applicable

Funding

The authors declare that no funds, grants and other support were received during the preparation of this manuscript.

Competing Interest

The Authors have no relevant financial or non-financial interest to disclose.

Author Contributions

Falowo Olayomi Abiodun and Olaiya Tomiwa Ayomiposi contributed to the study conception and design. Material preparation, data collection and analysis were performed by Falowo Olayomi Abiodun, Oladipo Babatunde, Oyekola Oluwaseun, Taiwo Abiola Ezekiel and Betiku Eriola. The first draft of the manuscript was written by Falowo Olayomi Abiodun and Oladipo Babatunde, and Oyekola Oluwaseun and Betiku Eriola commented on and proof-read the previous versions of the manuscript. All authors read and approved the final manuscript.

Availability of data and materials

The authors confirm that the data supporting the findings of this study are available within the article and its supplementary materials.

References

1. Abdullah, S. H. Y. S., Hanapi, N. H. M., Azid, A., Umar, R., Juahir, H., Khatoon, H. and Endut, A. (2017). A Review of Biomass-Derived Heterogeneous Catalyst for a Sustainable Biodiesel Production. *Renewable and Sustainable Energy Reviews,* 70: 1040-1051.
2. Ahmad, A., Yasin, N. M., Derek, C. and Lim, J. (2011). Microalgae as a Sustainable Energy Source for Biodiesel Production: A Review. *Renewable and Sustainable Energy Reviews,* 15: 584-593.
3. Akella, A., Saini, R. and Sharma, M. P. (2009). Social, Economical and Environmental Impacts of Renewable Energy Systems. *Renewable energy,* 34: 390-396.

4. AOAC (1990). Official Methods of Analysis of the Association of Official Analytical Chemists. *Official methods of analysis of the Association of Official Analytical Chemists.*
5. Balajii, M. and Niju, S. (2019). A Novel Biobased Heterogeneous Catalyst Derived from Musa Acuminata Peduncle for Biodiesel Production–Process Optimization Using Central Composite Design. *Energy Conversion and Management,* 189: 118-131.
6. Balajii, M. and Niju, S. (2020). Banana Peduncle–a Green and Renewable Heterogeneous Base Catalyst for Biodiesel Production from Ceiba Pentandra Oil. *Renewable energy,* 146: 2255-2269.
7. Betiku, E. and Ajala, S. O. (2014). Modeling and Optimization of Thevetia Peruviana (Yellow Oleander) Oil Biodiesel Synthesis Via Musa Paradisiacal (Plantain) Peels as Heterogeneous Base Catalyst: A Case of Artificial Neural Network Vs. Response Surface Methodology. *Industrial Crops and Products,* 53: 314-322.
8. Betiku, E., Akintunde, A. M. and Ojumu, T. V. (2016). Banana Peels as a Biobase Catalyst for Fatty Acid Methyl Esters Production Using Napoleon's Plume (Bauhinia Monandra) Seed Oil: A Process Parameters Optimization Study. *Energy,* 103: 797-806.
9. Betiku, E., Etim, A. O., Pereao, O. and Ojumu, T. V. (2017). Two-Step Conversion of Neem (Azadirachta Indica) Seed Oil into Fatty Methyl Esters Using a Heterogeneous Biomass-Based Catalyst: An Example of Cocoa Pod Husk. *Energy & Fuels,* 31: 6182-6193.
10. Bhatia, S. K., Gurav, R., Choi, T.-R., Kim, H. J., Yang, S.-Y., Song, H.-S., Park, J. Y., Park, Y.-L., Han, Y.-H. and Choi, Y.-K. (2020). Conversion of Waste Cooking Oil into Biodiesel Using Heterogenous Catalyst Derived from Cork Biochar. *Bioresource technology,* 302: 122872.
11. Deka, D. C. and Basumatary, S. (2011). High Quality Biodiesel from Yellow Oleander (Thevetia Peruviana) Seed Oil. *Biomass and bioenergy,* 35: 1797-1803.
12. Demirbaş, A. (1998). Fuel Properties and Calculation of Higher Heating Values of Vegetable Oils. *Fuel,* 77: 1117-1120.
13. Deora, P. S., Verma, Y., Muhal, R. A., Goswami, C. and Singh, T. (2021). Biofuels: An Alternative to Conventional Fuel and Energy Source. *Materials Today: Proceedings*.
14. Dhawane, S. H., Kumar, T. and Halder, G. (2016). Parametric Effects and Optimization on Synthesis of Iron (Ii) Doped Carbonaceous Catalyst for the Production of Biodiesel. *Energy Conversion and Management,* 122: 310-320.
15. Etim, A. O., Betiku, E., Ajala, S. O., Olaniyi, P. J. and Ojumu, T. V. (2018). Potential of Ripe Plantain Fruit Peels as an Ecofriendly Catalyst for Biodiesel Synthesis: Optimization by Artificial Neural Network Integrated with Genetic Algorithm. *Sustainability,* 10: 707.
16. Fadara, O. A., Falowo, O. A., Ojumu, T. V. and Betiku, E. (2021). Process Optimization of Microwave Irradiation-Aided Transesterification of Kariya Seed Oil by Taguchi Orthogonal Array: Pawpaw Trunk as a Novel Biocatalyst. *Biofuels, Bioproducts and Biorefining*.
17. Falowo, O. A., Ojumu, T. V., Pereao, O. and Betiku, E. (2020). Sustainable Biodiesel Synthesis from Honne-Rubber-Neem Oil Blend with a Novel Mesoporous Base Catalyst Synthesized from a Mixture of Three Agrowastes. *Catalysts,* 10: 190.
18. Falowo, O. A., Oloko-Oba, M. I. and Betiku, E. (2019). Biodiesel Production Intensification Via Microwave Irradiation-Assisted Transesterification of Oil Blend Using Nanoparticles from Elephant-Ear Tree Pod Husk

as a Base Heterogeneous Catalyst. *Chemical Engineering and Processing-Process Intensification,* 140: 157-170.

19. Gebremariam, S. and Marchetti, J. (2018). Economics of Biodiesel Production. *Energy Conversion and Management,* 168: 74-84.
20. Gohain, M., Devi, A. and Deka, D. (2017). Musa Balbisiana Colla Peel as Highly Effective Renewable Heterogeneous Base Catalyst for Biodiesel Production. *Industrial Crops and Products,* 109: 8-18.
21. Gohain, M., Laskar, K., Paul, A. K., Daimary, N., Maharana, M., Goswami, I. K., Hazarika, A., Bora, U. and Deka, D. (2020). Carica Papaya Stem: A Source of Versatile Heterogeneous Catalyst for Biodiesel Production and C–C Bond Formation. *Renewable energy,* 147: 541-555.
22. Huang, G., Chen, F., Wei, D., Zhang, X. and Chen, G. (2010). Biodiesel Production by Microalgal Biotechnology. *Applied energy,* 87: 38-46.
23. Hwang, N. and Barron, A. R. (2011). Bet Surface Area Analysis of Nanoparticles. *The Connexions project,* 1-11.
24. Konwar, L. J., Das, R., Thakur, A. J., Salminen, E., Mäki-Arvela, P., Kumar, N., Mikkola, J.-P. and Deka, D. (2014). Biodiesel Production from Acid Oils Using Sulfonated Carbon Catalyst Derived from Oil-Cake Waste. *Journal of Molecular Catalysis A: Chemical,* 388: 167-176.
25. Krisnangkura, K. (1986). A Simple Method for Estimation of Cetane Index of Vegetable Oil Methyl Esters. *Journal of the American Oil Chemists Society,* 63: 552-553.
26. Kumar, A. and Sharma, S. (2011). Potential Non-Edible Oil Resources as Biodiesel Feedstock: An Indian Perspective. *Renewable and Sustainable Energy Reviews,* 15: 1791-1800.
27. Loizides, M. I., Loizidou, X. I., Orthodoxou, D. L. and Petsa, D. (2019). Circular Bioeconomy in Action: Collection and Recycling of Domestic Used Cooking Oil through a Social, Reverse Logistics System. *Recycling,* 4: 16.
28. Ma, F. and Hanna, M. A. (1999). Biodiesel Production: A Review. *Bioresource technology,* 70: 1-15.
29. Marchetti, J., Miguel, V. and Errazu, A. (2007). Possible Methods for Biodiesel Production. *Renewable and Sustainable Energy Reviews,* 11: 1300-1311.
30. Mustata, F. and Bicu, I. (2014). The Optimization of the Production of Methyl Esters from Corn Oil Using Barium Hydroxide as a Heterogeneous Catalyst. *Journal of the American Oil Chemists' Society,* 91: 839-847.
31. Naderi, M. (2015). Surface Area: Brunauer–Emmett–Teller (Bet) *Progress in Filtration and Separation* (pp. 585-608): Elsevier.
32. Niju, S., Ajieth Kanna, S. K., Ramalingam, V., Satheesh Kumar, M. and Balajii, M. (2019). Sugarcane Bagasse Derived Biochar–a Potential Heterogeneous Catalyst for Transesterification Process. *Energy Sources, Part A: Recovery, Utilization, and Environmental Effects,* 1-12.
33. Odude, V. O., Adesina, A. J., Oyetunde, O. O., Adeyemi, O. O., Ishola, N. B., Etim, A. O. and Betiku, E. (2017). Application of Agricultural Waste-Based Catalysts to Transesterification of Esterified Palm Kernel Oil into Biodiesel: A Case of Banana Fruit Peel Versus Cocoa Pod Husk. *Waste and Biomass Valorization,* 1-12.
34. Oladipo, B. and Betiku, E. (2020). Optimization and Kinetic Studies on Conversion of Rubber Seed (Hevea Brasiliensis) Oil to Methyl Esters over a Green Biowaste Catalyst. *Journal of environmental management,* 268: 110705.

35. Oladipo, B., Ojumu, T. and Betiku, E. (2018). Potential of Pawpaw Peels as a Base Heterogeneous Catalyst for Biodiesel Production: Modeling and Optimization Studies. *Niger Soc Chem Eng,* 1-11.
36. Oladipo, B., Ojumu, T. V., Latinwo, L. M. and Betiku, E. (2020). Pawpaw (Carica Papaya) Peel Waste as a Novel Green Heterogeneous Catalyst for Moringa Oil Methyl Esters Synthesis: Process Optimization and Kinetic Study. *Energies,* 13: 5834.
37. Olagbende, O. H., Falowo, O. A., Latinwo, L. M. and Betiku, E. (2021). Esterification of Khaya Senegalensis Seed Oil with a Solid Heterogeneous Acid Catalyst: Modeling, Optimization, Kinetic and Thermodynamic Studies. *Cleaner Engineering and Technology,* 100200.
38. Olatundun, E. A., Borokini, O. O. and Betiku, E. (2020). Cocoa Pod Husk-Plantain Peel Blend as a Novel Green Heterogeneous Catalyst for Renewable and Sustainable Honne Oil Biodiesel Synthesis: A Case of Biowastes-to-Wealth. *Renewable energy,* 166: 163-175.
39. Oraegbunam, J. C., Oladipo, B., Falowo, O. A. and Betiku, E. (2020). Clean Sandbox (Hura Crepitans) Oil Methyl Esters Synthesis: A Kinetic and Thermodynamic Study through Ph Monitoring Approach. *Renewable energy*.
40. Pavlović, S. M., Marinković, D. M., Kostić, M. D., Janković-Častvan, I. M., Mojović, L. V., Stanković, M. V. and Veljković, V. B. (2020). A Cao/Zeolite-Based Catalyst Obtained from Waste Chicken Eggshell and Coal Fly Ash for Biodiesel Production. *Fuel,* 267: 117171.
41. Predojević, Z. J. (2008). The Production of Biodiesel from Waste Frying Oils: A Comparison of Different Purification Steps. *Fuel,* 87: 3522-3528.
42. Qiu, F., Li, Y., Yang, D., Li, X. and Sun, P. (2011). Biodiesel Production from Mixed Soybean Oil and Rapeseed Oil. *Applied energy,* 88: 2050-2055.
43. Sharma, M., Khan, A. A., Puri, S. and Tuli, D. (2012). Wood Ash as a Potential Heterogeneous Catalyst for Biodiesel Synthesis. *Biomass and bioenergy,* 41: 94-106.
44. Sivarethinamohan, S., Hanumanthu, J. R., Gaddam, K., Ravindiran, G. and Alagumalai, A. (2022). Towards Sustainable Biodiesel Production by Solar Intensification of Waste Cooking Oil and Engine Parameter Assessment Studies. *Science of the Total Environment,* 804: 150236.
45. Soji-Adekunle, A. R., Asere, A. A., Ishola, N. B., Oloko-Oba, I. M. and Betiku, E. (2018). Modeling of Synthesis of Waste Cooking Oil Methyl Esters by Artificial Neural Network and Response Surface Methodology. *International Journal of Ambient Energy,* 1-34.
46. Tariq, M., Ali, S., Ahmad, F., Ahmad, M., Zafar, M., Khalid, N. and Khan, M. A. (2011). Identification, Ft-Ir, Nmr (1h and 13c) and Gc/Ms Studies of Fatty Acid Methyl Esters in Biodiesel from Rocket Seed Oil. *Fuel Processing Technology,* 92: 336-341.
47. Zhang, C.-Y., Shao, W.-L., Zhou, W.-X., Liu, Y., Han, Y.-Y., Zheng, Y. and Liu, Y.-J. (2019). Biodiesel Production by Esterification Reaction on K+ Modified Mgal-Hydrotalcites Catalysts. *Catalysts,* 9: 742.

Figures

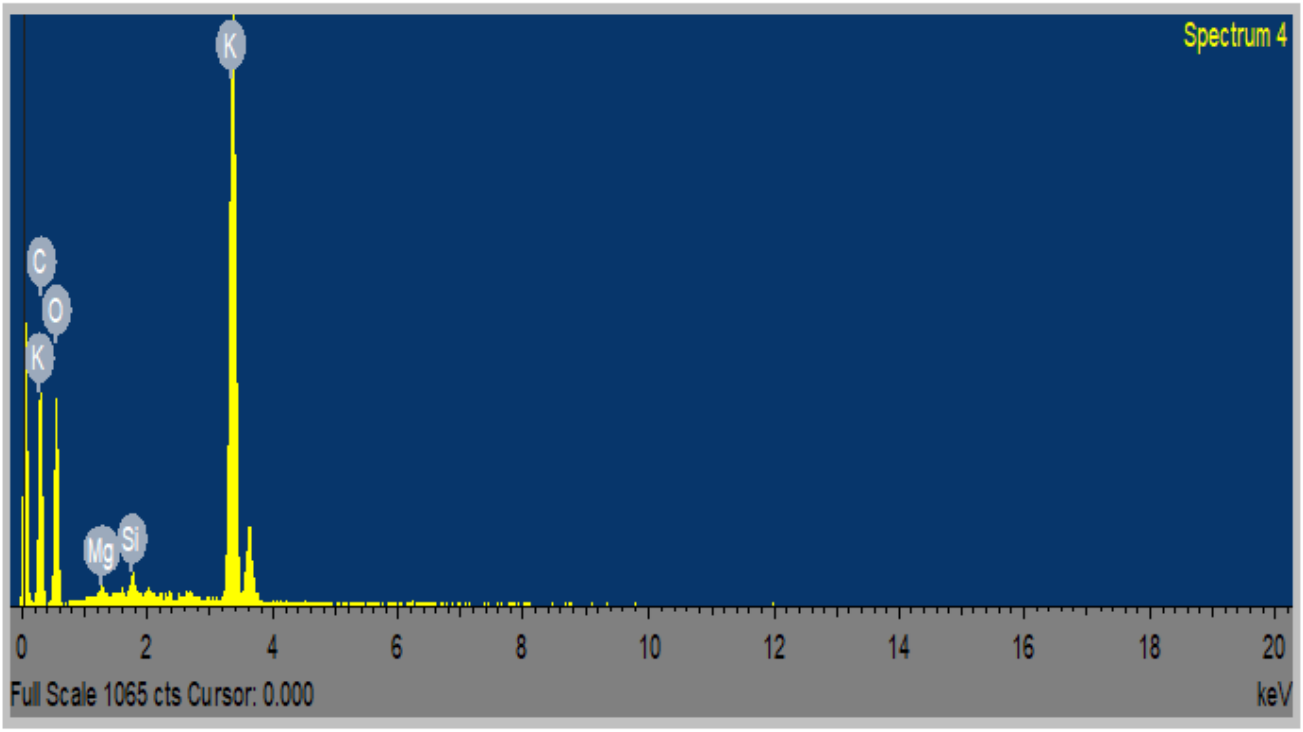

Figure 1

Pictograph of EDX of CRUPA

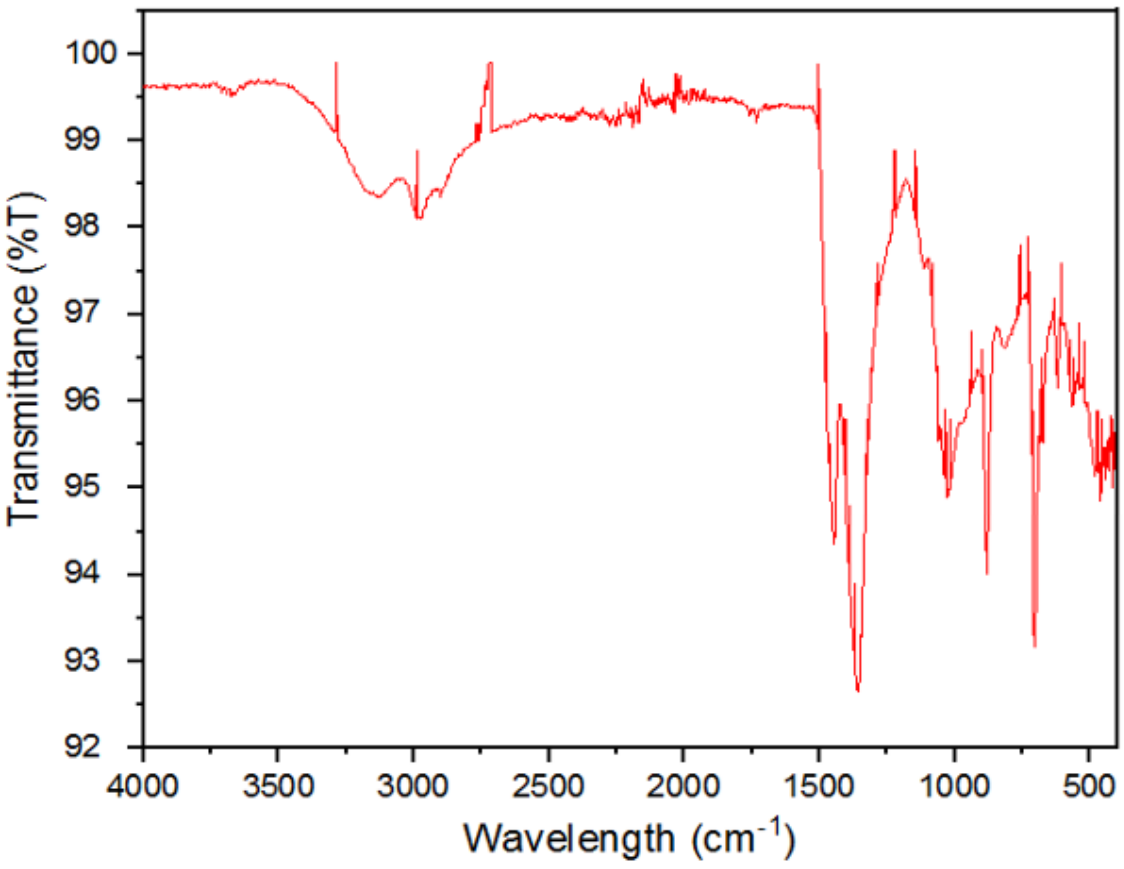

Figure 2

FT-IR spectrum of CRUPA

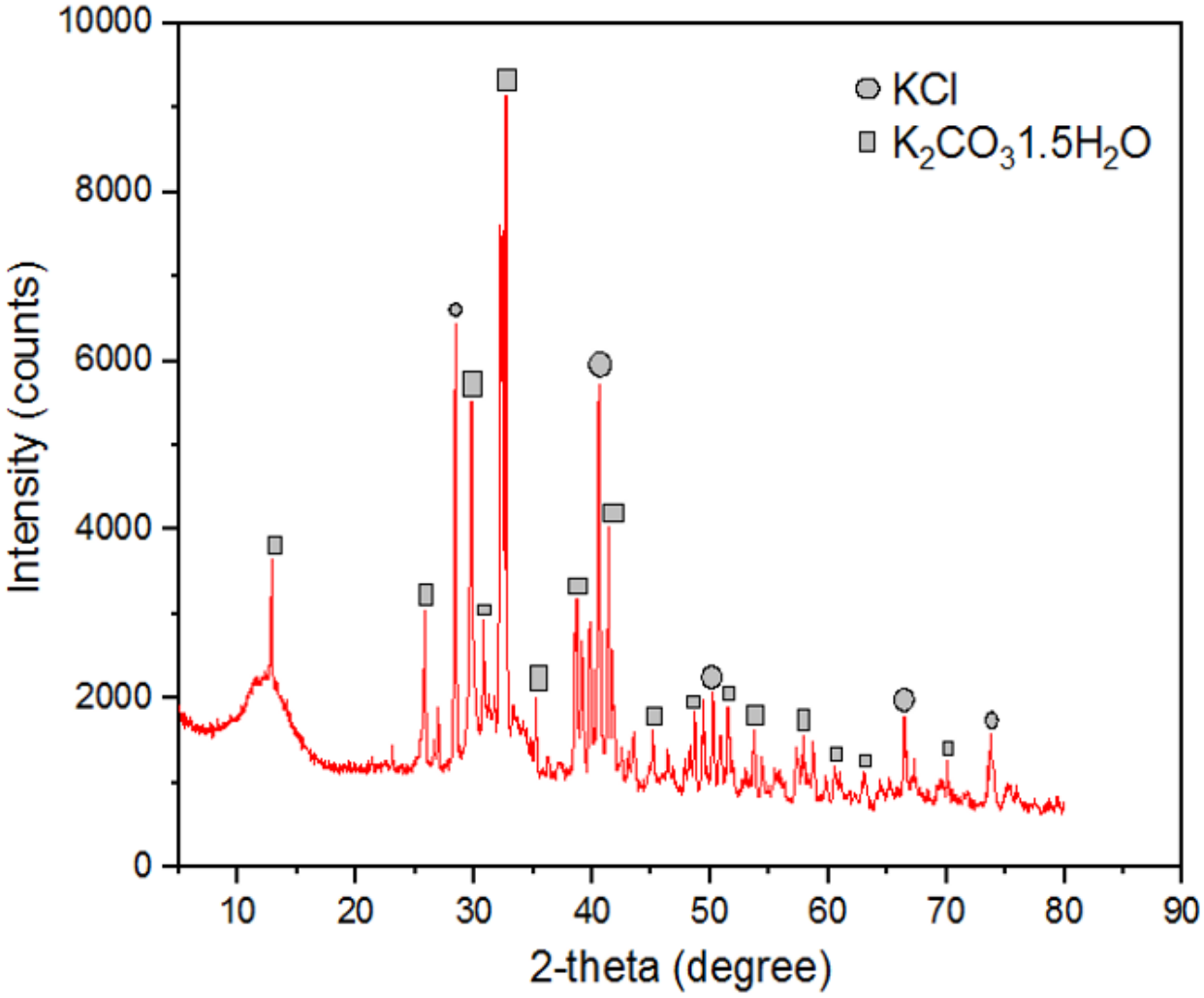

Figure 3

XRD diffractogram of CRUPA

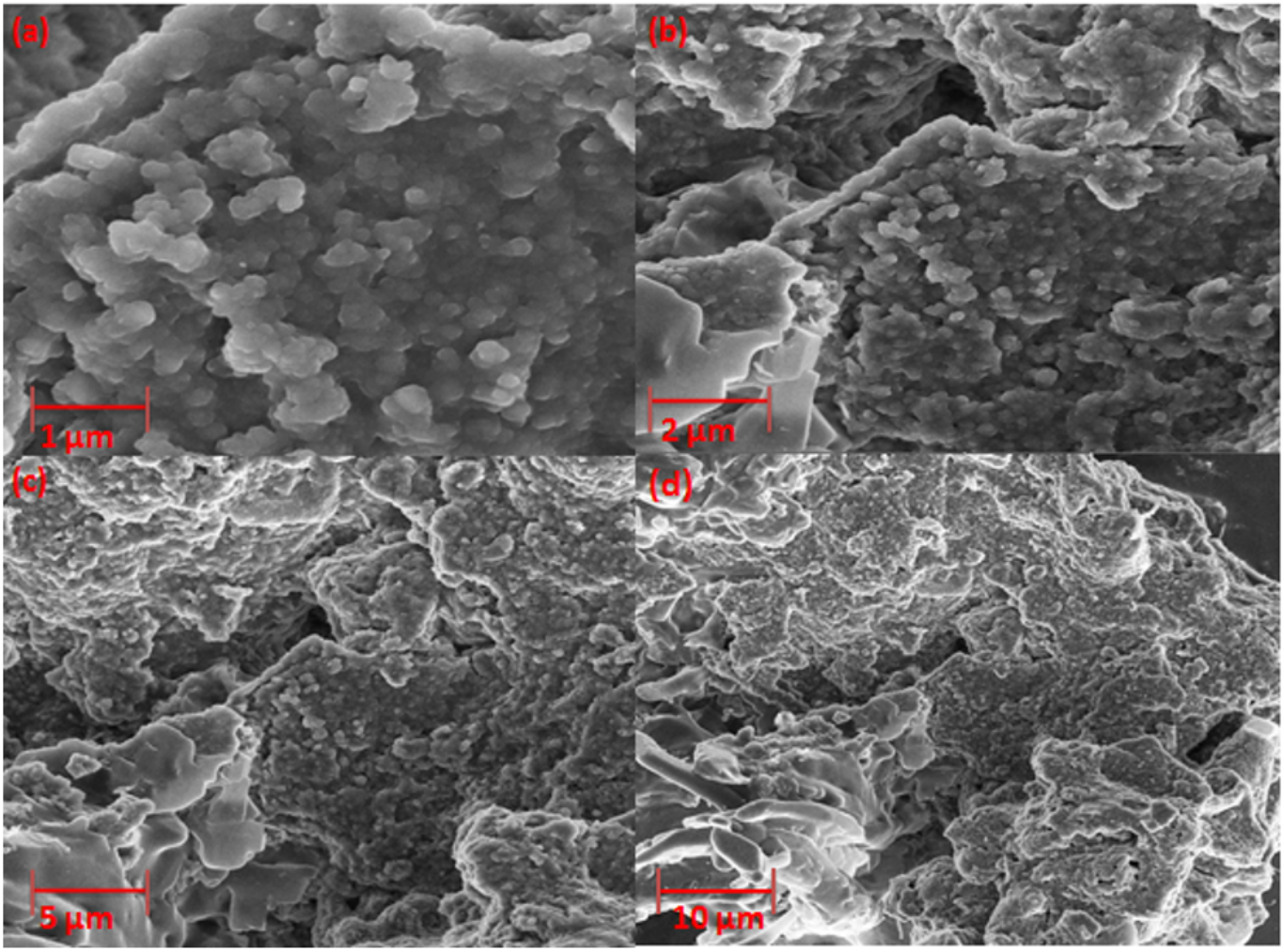

Figure 4

(a-d): SEM images of CRUPA

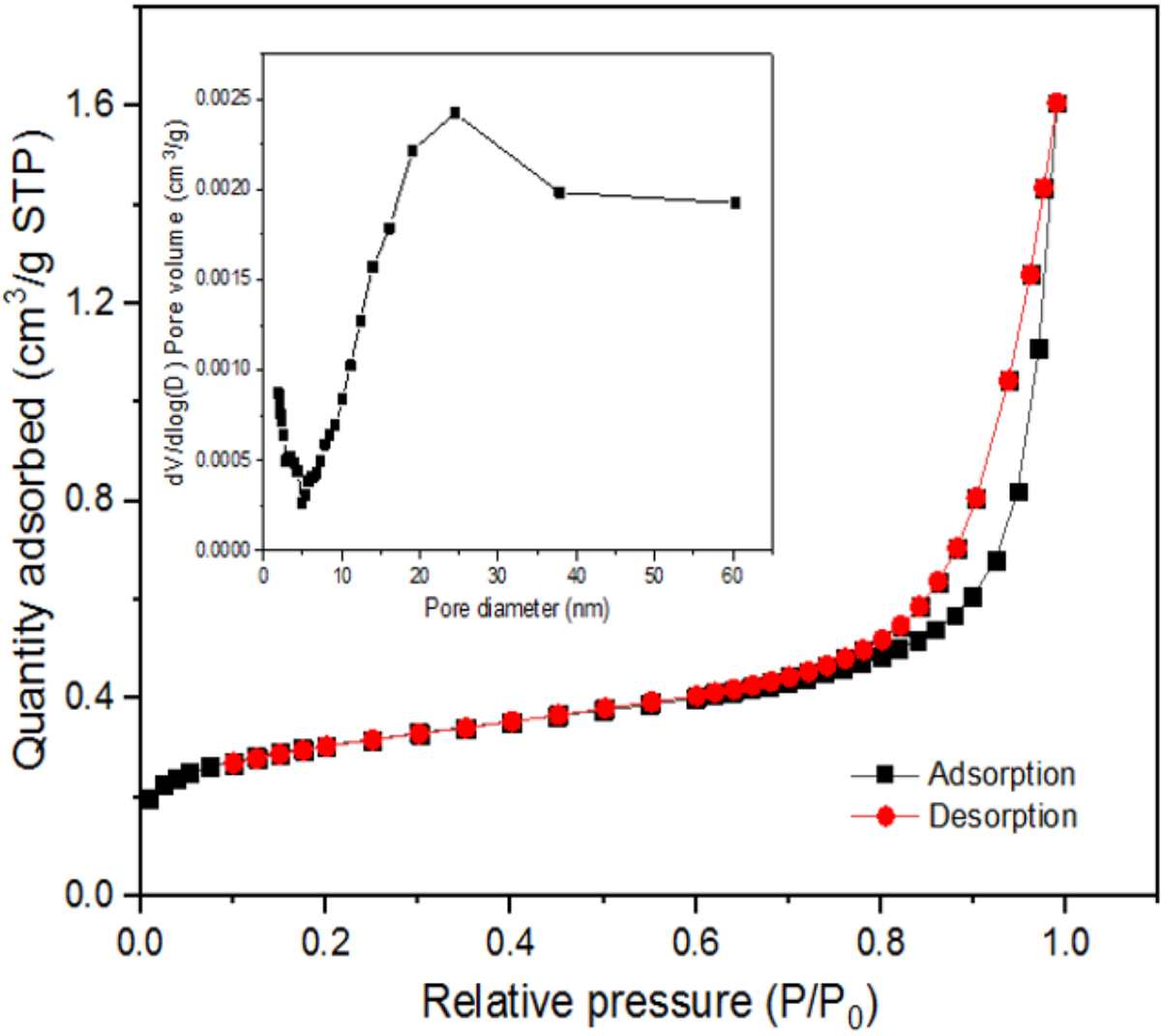

Figure 5

BET adsorption isotherm and BJH pore-size distribution (inset) of CRUPA

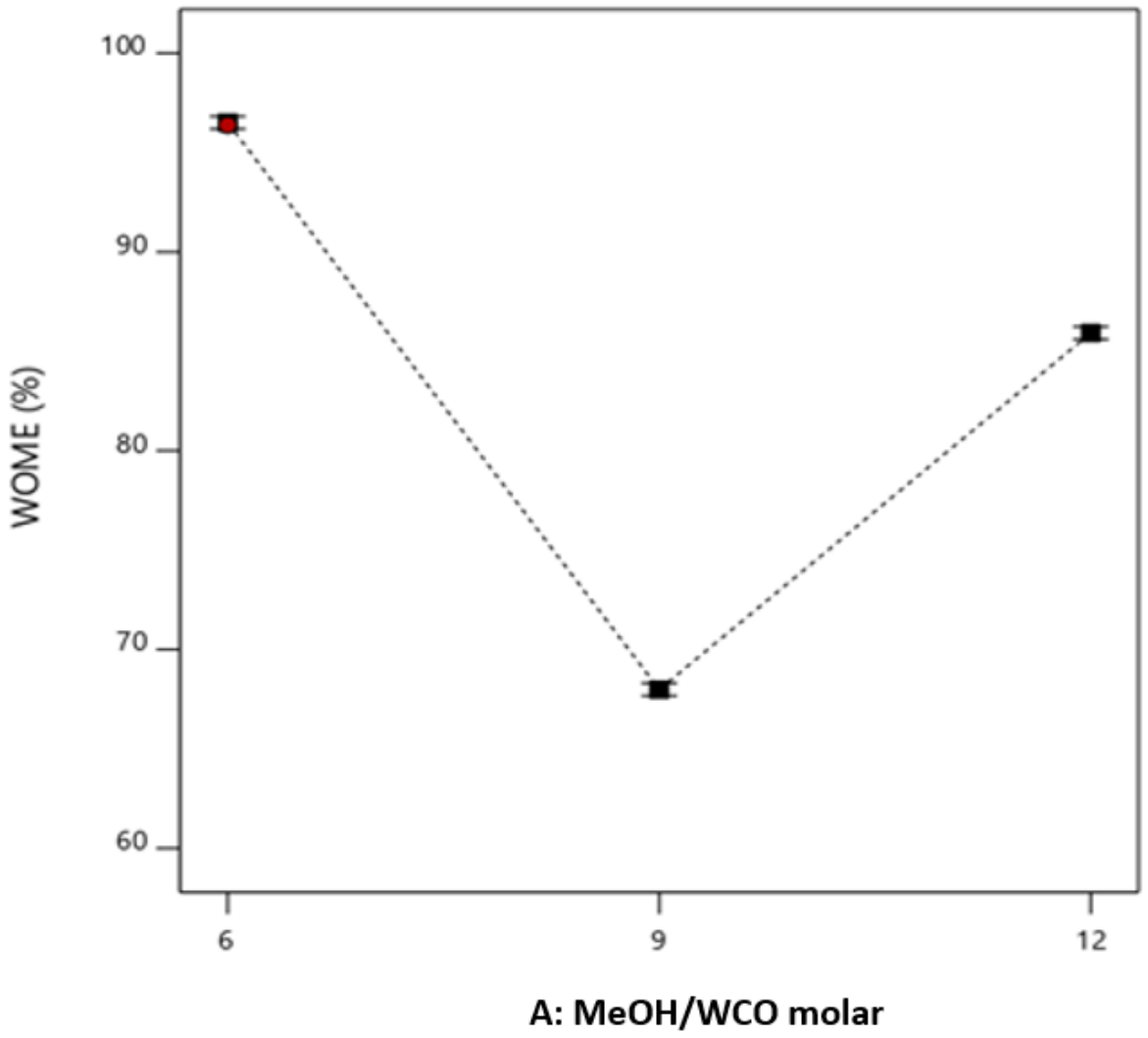

Figure 6

Plot of methanol/WCO molar ratio effect on WOME yield (wt.%)

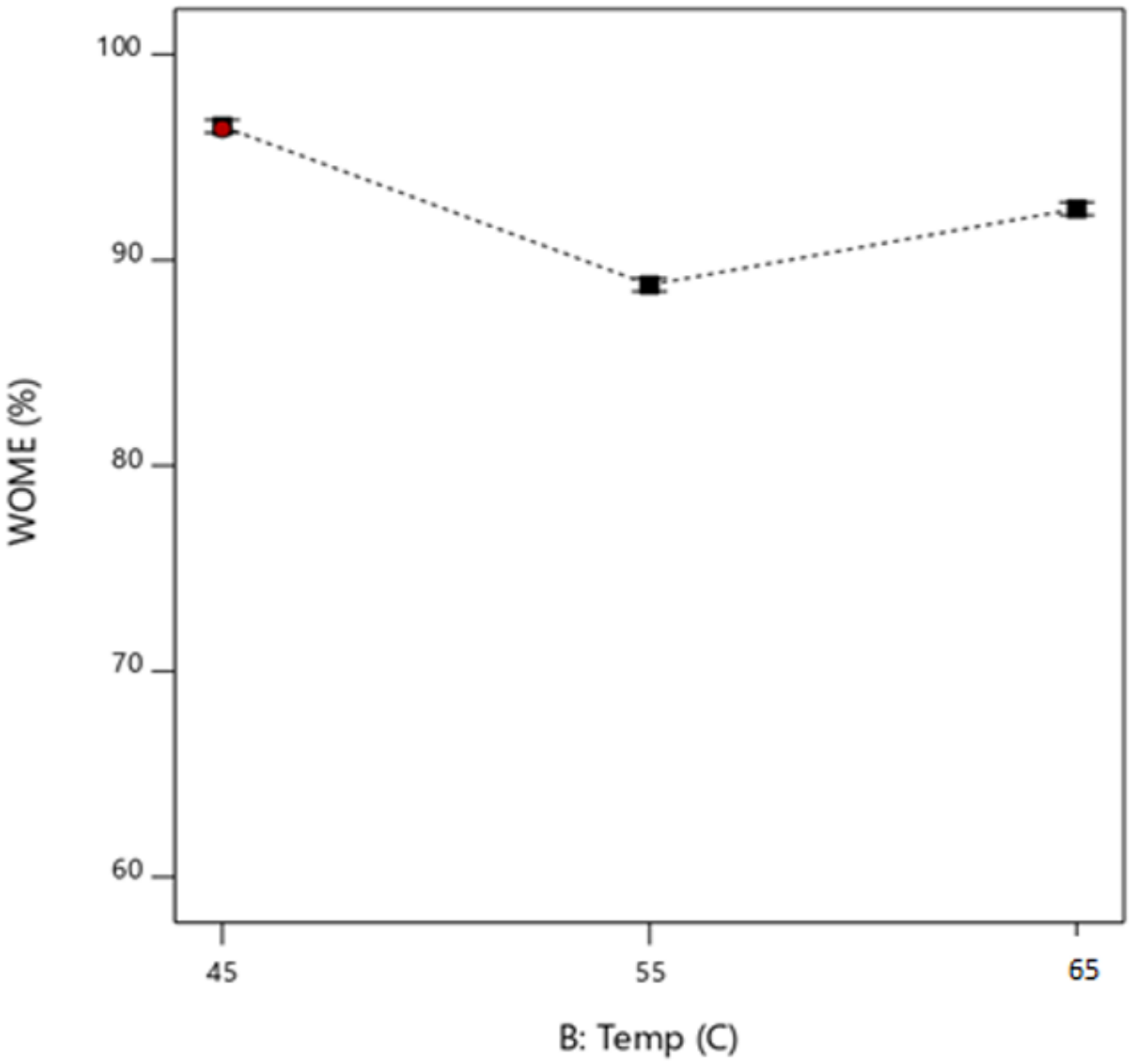

Figure 7

Influence of temperature on WOME yield (wt.%)

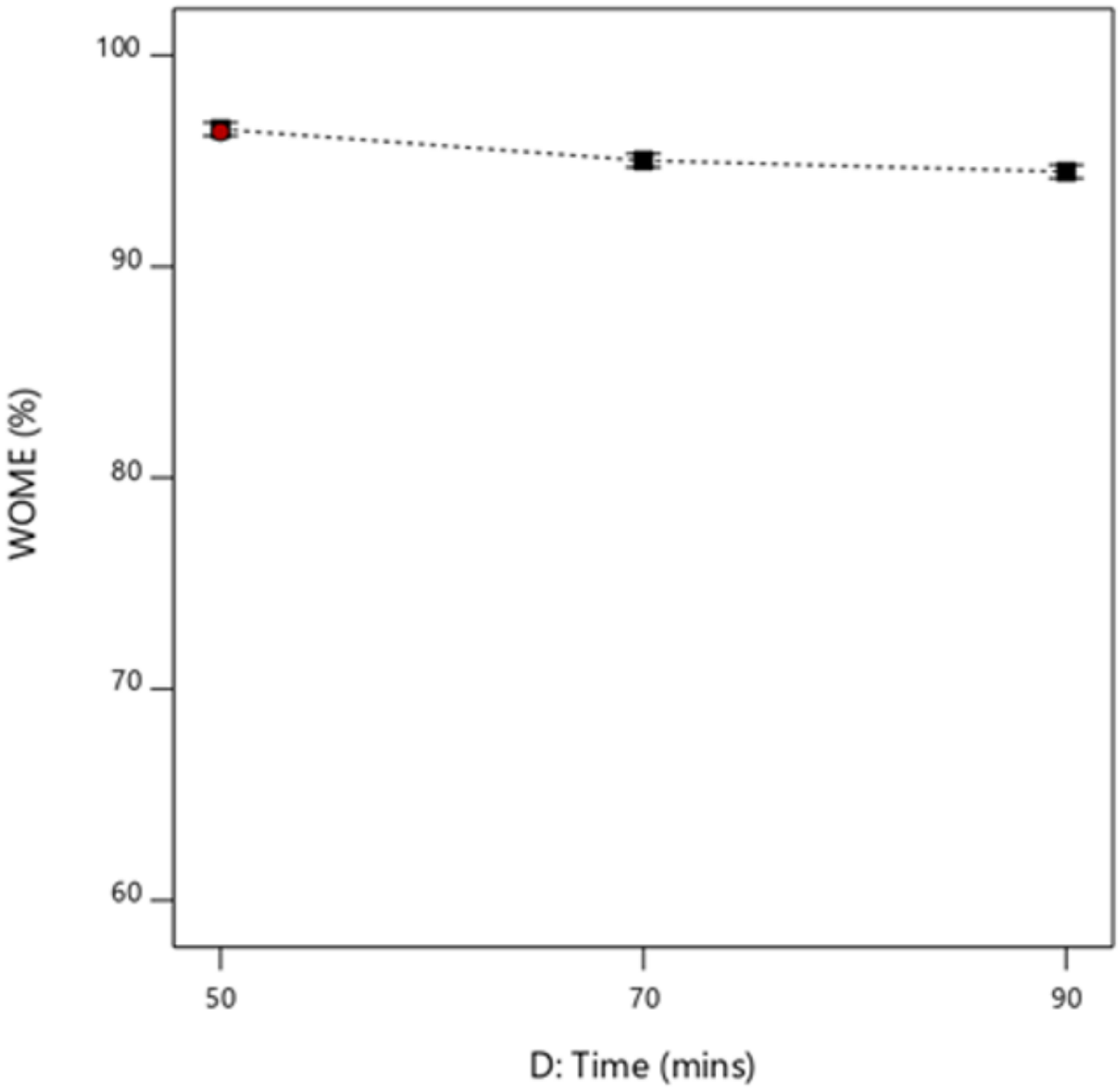

Figure 8

Influence of reaction time on WOME yield (wt.%)

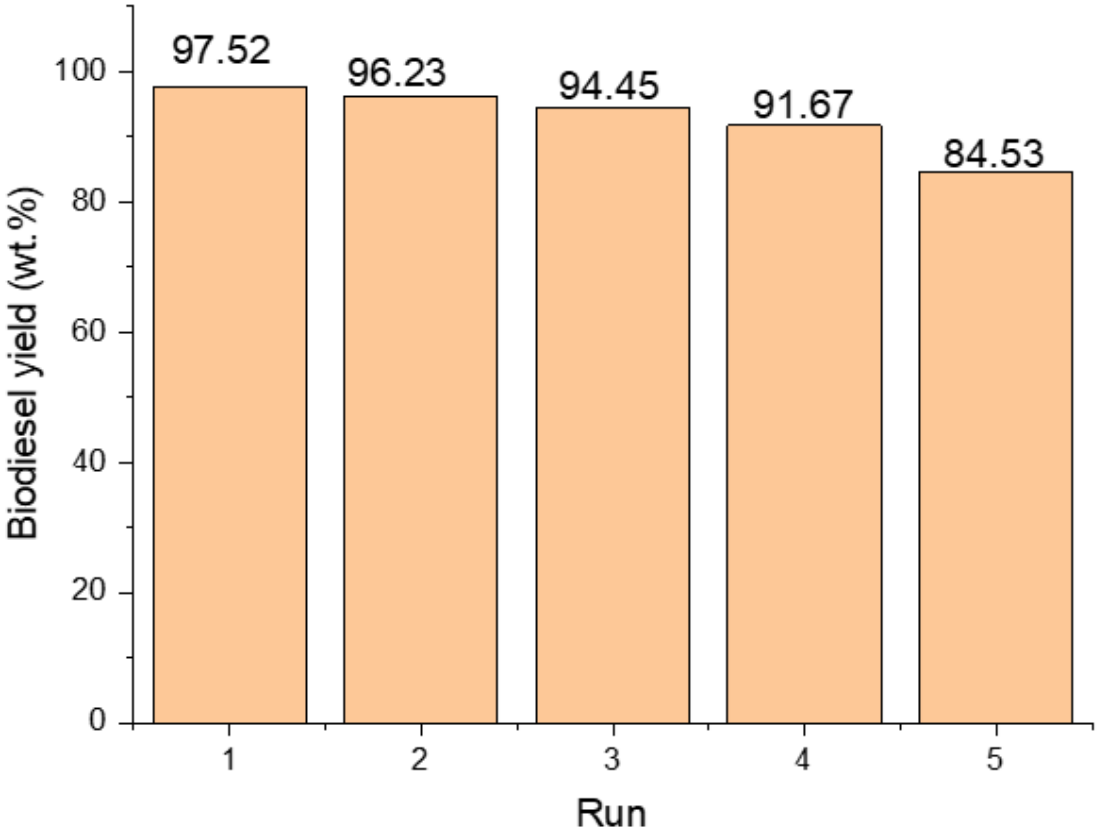

Figure 9

Reusability results of CRUPA

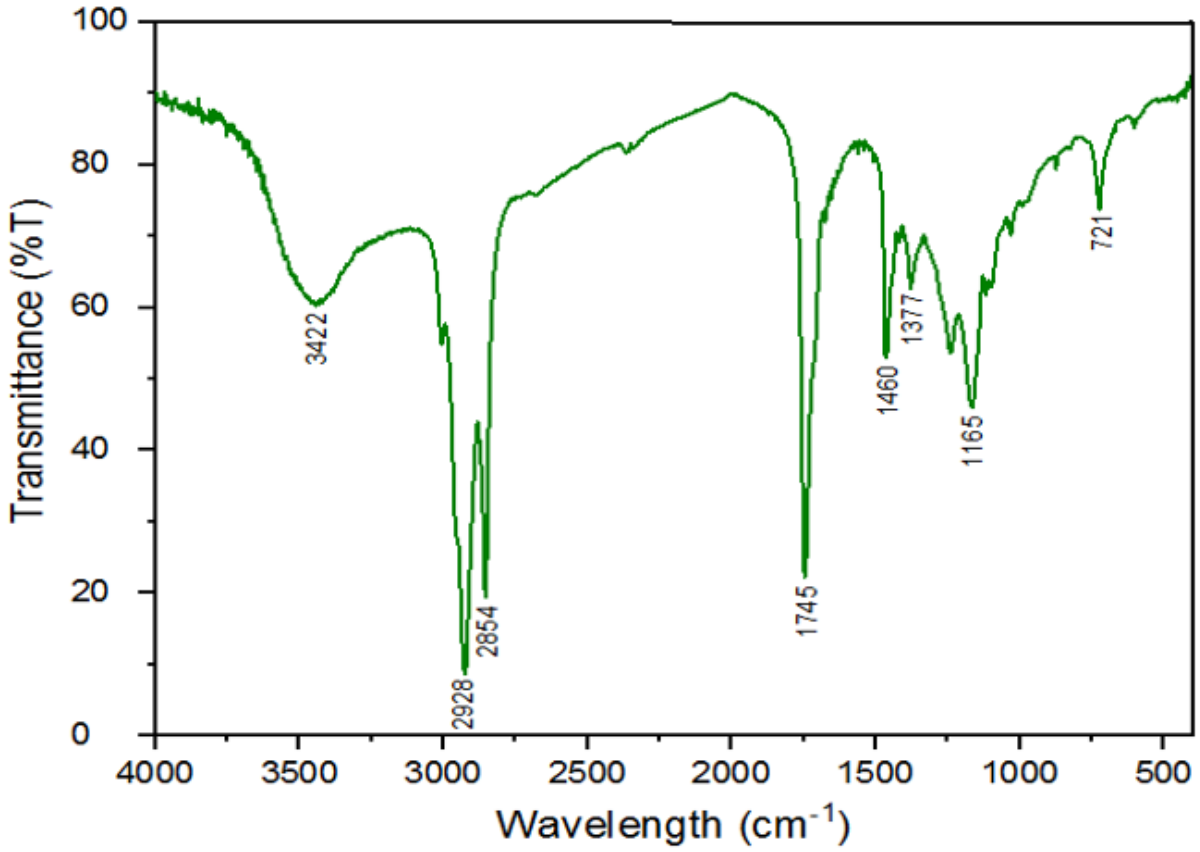

Figure 10

FT-IR spectrum of WOME

Supplementary Files

This is a list of supplementary files associated with this preprint. Click to download.

- TS1.txt
- TS1noFenps.pdf
- TSI1.tif
- TSI2.tif
- TSI3.tif
- TSI4.tif
- bgndTS1.txt